scientific reports

Check for updates

OPEN

Dermal macrophages control tactile perception under physiological conditions via NGF signaling

Tatsuhide Tanaka[1]✉, Ayami Isonishi[1], Mitsuko Banja[1], Rikuto Yamamoto[2], Masaki Sonobe[1], Emiko Okuda-Ashitaka[2], Hidemasa Furue[3], Hiroaki Okuda[4], Kouko Tatsumi[1] & Akio Wanaka[1]

We demonstrated previously that sorting nexin 25 (SNX25) in nerve-associated macrophages plays critical roles in pain sensation by regulating tissue NGF content under both physiological and neuropathic conditions. In the present study, we apply the SNX25–NGF paradigm to tactile perception by showing that *Snx25*$^{+/-}$ mice or macrophage-specific *Snx25* conditional knock-out (mcKO) mice had weaker responses to tactile stimuli in normal conditions. *Snx25* mcKO mice responded poorly to transcutaneous electrical stimuli at a frequency of 5 Hz (C fiber responses), but normally to stimuli at a frequency of 250 Hz (Aδ fiber responses) or of 2000 Hz (Aβ fiber responses). CX3CR1-positive dermal macrophages were frequently found near calcitonin gene–related peptide (CGRP)- positive nerves and, less frequently, tyrosine hydroxylase (TH)-positive nerves. We confirmed that the tissue content of NGF was lower in *Snx25* mcKO mice than in wild-type mice, and in turn, dermal NGF injection restored tactile sensitivity in *Snx25*$^{+/-}$ mice and *Snx25* mcKO mice to normal levels. These results indicate that CGRP-positive C-nociceptors (possibly also TH-positive C-LTMRs) associated dermal macrophages control tactile perception by producing NGF and secreting it into the dermis.

Keywords Dermal macrophage, Tactile perception, SNX25, NGF

The skin is frequently stressed by mechanical trauma. Sensory stimuli impinging on skin are encoded by peripheral sensory neurons that can be classified into low-threshold mechanoreceptors (LTMRs), which detect innocuous tactile stimuli, and high-threshold mechanoreceptors (HTMRs) nociceptors, which respond to harmful mechanical stimuli[1,2]. HTMRs are a broad category of mechanonociceptive sensory neurons that are optimally excited by noxious mechanical stimuli. HTMRs include Aδ and C free nerve endings. Aδ-HTMRs are thought to mediate fast mechanical pain and can be further divided into fibers that respond to either noxious heat or cold stimuli. On the other hand, C-HTMRs respond solely to mechanical stimuli[3]. Based on action potential conduction velocity, cutaneous LTMRs are classified into Aβ-, Aδ-, and C-LTMRs [1]. C-LTMRs, the slowest-conducting mechanoreceptor subtype, make up a large fraction of dorsal root ganglion (DRG) neurons (~ 15–30%)[4,5]. In mice, a subpopulation of C-LTMRs can be identified based on its expression of tyrosine hydroxylase (TH) and VGLUT3[5], and these neurons respond to gentle mechanical force.

We previously discovered *sorting nexin 25* (*Snx25*) as a pain-modulating gene[6]. SNX family members are involved in membrane trafficking, cell signaling, membrane remodeling, and organelle motility[7]. We showed that SNX25 in nerve-associated dermal macrophages activates nerve growth factor (NGF) production by inhibiting ubiquitin-mediated degradation of Nrf2, one of the key transcription factors that activates *Ngf* mRNA transcription, and modulates acute pain sensing under both normal and painful conditions via NGF/TrkA signaling[6]. These findings indicate that macrophage-to-neuron signaling is important in pain processing even in naïve skin as well as in neuropathic or inflammatory situations. Pain and touch are intricately related, therefore insights into the processing of pain and weak mechanical responses in physiological environments is important. Nerve–macrophage interactions may cover from pathological pain sensation to tactile perception in a seamless fashion. We aim to elucidate the molecular mechanism of tactile sensation as an extension of pain research.

[1]Department of Anatomy and Neuroscience, Nara Medical University, Kashihara, Nara, Japan. [2]Department of Biomedical Engineering, Osaka Institute of Technology, Osaka, Japan. [3]Department of Neurophysiology, Hyogo Medical University, Nishinomiya, Hyogo, Japan. [4]Department of Functional Morphology, Faculty of Pharmacy, Osaka Medical and Pharmaceutical University, Takatsuki, Osaka, Japan. ✉email: ttanaka@naramed-u.ac.jp

Understanding how our sensory processing mechanisms can be modulated physiologically promises to help researchers and clinicians find new ways to alleviate the suffering of chronic pain patients.

NGF is important for generation of pain and in hyperalgesia in diverse pain states[8]. In addition to enhancing the activity of nociceptive ion channels to promote rapid depolarization and sensitization, NGF also mediates changes in gene expression and membrane protein localization, both of which contribute to increased sensory neuron excitability[9]. NGF signaling is the master regulator for expression of functional genes in C fibers in addition to its role in survival[10]. Although the level of NGF should be maintained within an optimal range for sensing the normal environment and the mechanisms underlying its regulation remain elusive, we have demonstrated that dermal macrophages are one of the main sources of tissue NGF[6]. Accordingly, we hypothesized that SNX25 and NGF may also have important roles in tactile perception under physiological condition as well as in pain sensation. We demonstrated that dermal NGF injection restored tactile sensitivity in *Snx25*$^{+/-}$ mice and *Snx25* mcKO mice to normal levels. We also showed that CX3CR1-positive dermal macrophages were frequently associated with CGRP-positive C-nociceptors and TH-positive C-LTMRs. These results indicate that CGRP- and TH-positive C fiber-associated dermal macrophages control tactile perception by producing NGF and secreting it into the dermis.

Results

Snx25$^{+/-}$ mice show a tactile-insensitive phenotype

We previously demonstrated that *Snx25*$^{+/-}$ mice and *Snx25* mcKO mice had reduced pain responses under both normal and pain-inducing conditions[6]. Here, to investigate the roles of SNX25 in tactile sensation, we first examined the responses to low-pressure punctate stimuli in *Snx25*$^{+/-}$ and WT mice. *Snx25*$^{-/-}$ mice are embryonic lethal, and therefore we used SNX25 heterozygotes in our experiments. *Snx25*$^{+/-}$ mice responded more weakly than WT mice (Fig. 1a), suggesting that SNX25 is involved in innocuous tactile sensitivity. Many mechanosensory transduction channels have been proposed, and reported to cooperate with each other in the regulation of touch and pain sensation[11,12] We detected reduced mRNA levels of mechanosensory factors including *Trpv2*, *Trpc1*, and *Scn10a* in *Snx25*$^{+/-}$ DRGs (Fig. 1b). These data indicate that the touch-insensitive phenotype of the *Snx25*$^{+/-}$ mice was due to reduced levels of mechanosensory factors (*Trpv2*, *Trpc1*, and *Scn10a*) in the peripheral sensory neurons.

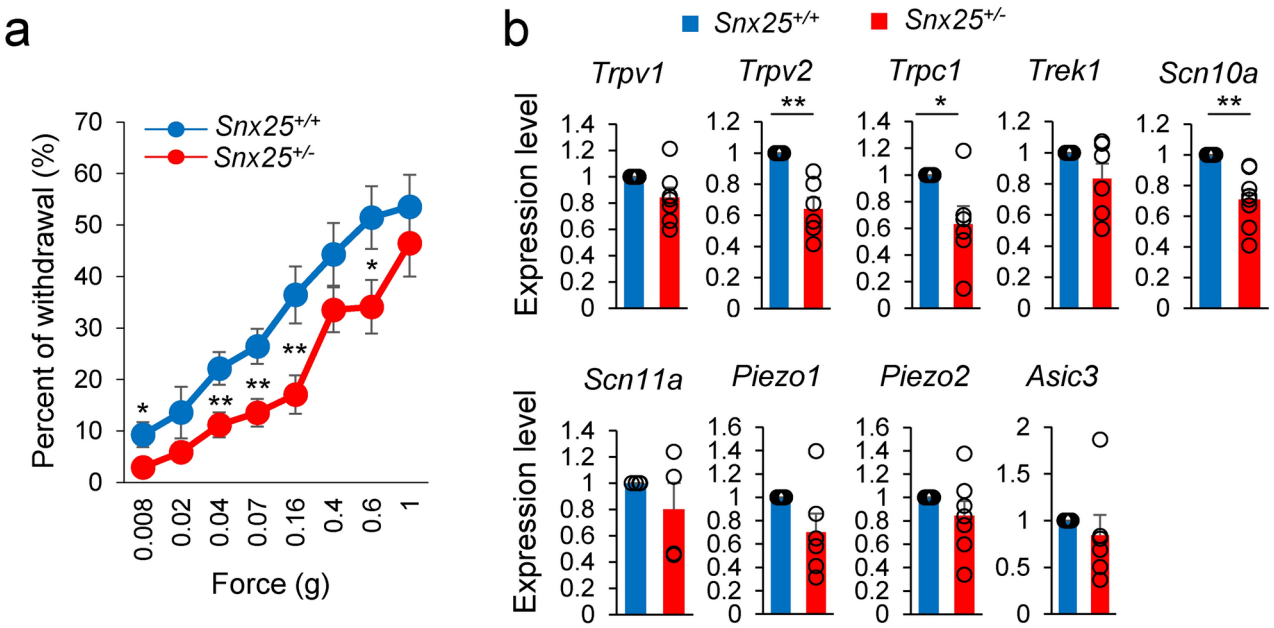

Fig. 1. *Snx25*$^{+/-}$ mice show a tactile-insensitive phenotype. (**a**) Fine tactile sensitivity was examined with von Frey filaments whose mechanical pressure ranged from 0.008 g to 1 g. When the plantar surface of the hind paw was stimulated for 1 s with these filaments, withdrawal immediately after stimulus was considered as a positive response. The percentage of positive responses in 10 time stimulations with each filament was measured. The percentages of withdrawal (positive response) to innocuous low-pressure stimuli were plotted (WT: n = 14; *Snx25*$^{+/-}$: n = 18). X-axis values indicate target forces of von Frey filaments. 0.008g; $p = 0.027$, 0.04g; $p = 0.009$, 0.07g; $p = 0.005$, 0.16g; $p = 0.005$, 0.6g; $p = 0.038$. (**b**) mRNA expression levels for mechanosensory factors in DRG of *Snx25*$^{+/-}$ mice were significantly lower than those of WT mice (WT: n = 4–8; *Snx25*$^{+/-}$: n = 4–8). *Trpv2*; $p = 0.004$, *Trpc1*; $p = 0.042$. $^{*}p < 0.05$, $^{**}p < 0.01$, n.s., not significant. Results are represented as mean ± SEM. Statistical analyses were performed using the Student's *t*-test (**a**) or Welch's *t*-test (**b**).

Snx25 cKO in macrophages yields a tactile-insensitive phenotype

A recent study demonstrated that Lyve1^{lo} MHC-II^{hi} CX3CR1^{hi} macrophages preferentially colocalize with peripheral nerves[13] and we demonstrated that nerve-associated macrophages modulate mechanical pain sensation[6]. To further target the nerve-associated macrophages, we crossed *Snx25*$^{fl/fl}$ mice with *Cx3cr1*$^{CreERT2/WT}$ mice to generate mice with a conditional deletion of SNX25 in monocytes and macrophages (hereafter named *Snx25* mcKO mice). We administered 0.05% tamoxifen (TAM) orally for 2 weeks, a method known to induce efficient recombination [14,15]. As in the *Snx25*$^{+/-}$ mice, *Snx25* mcKO mice exhibited reduced tactile responses to innocuous mechanical stimuli (Fig. 2a). Unlike tissue-resident macrophages (e.g., microglia in the brain, Langerhans cells in the epidermis), dermal macrophages in the skin have been shown to be derived from bone marrow (BM) and to turn over [6,16,17]. To gain insight into the contribution of BM-derived dermal macrophages to tactile sensation, we made BM-chimeric mice by cross-transplanting WT and *Snx25* mcKO mice BM (Fig. 2b). In this BM transplantation (BMT) experiment, TAM treatment was performed from 1 to 3 weeks

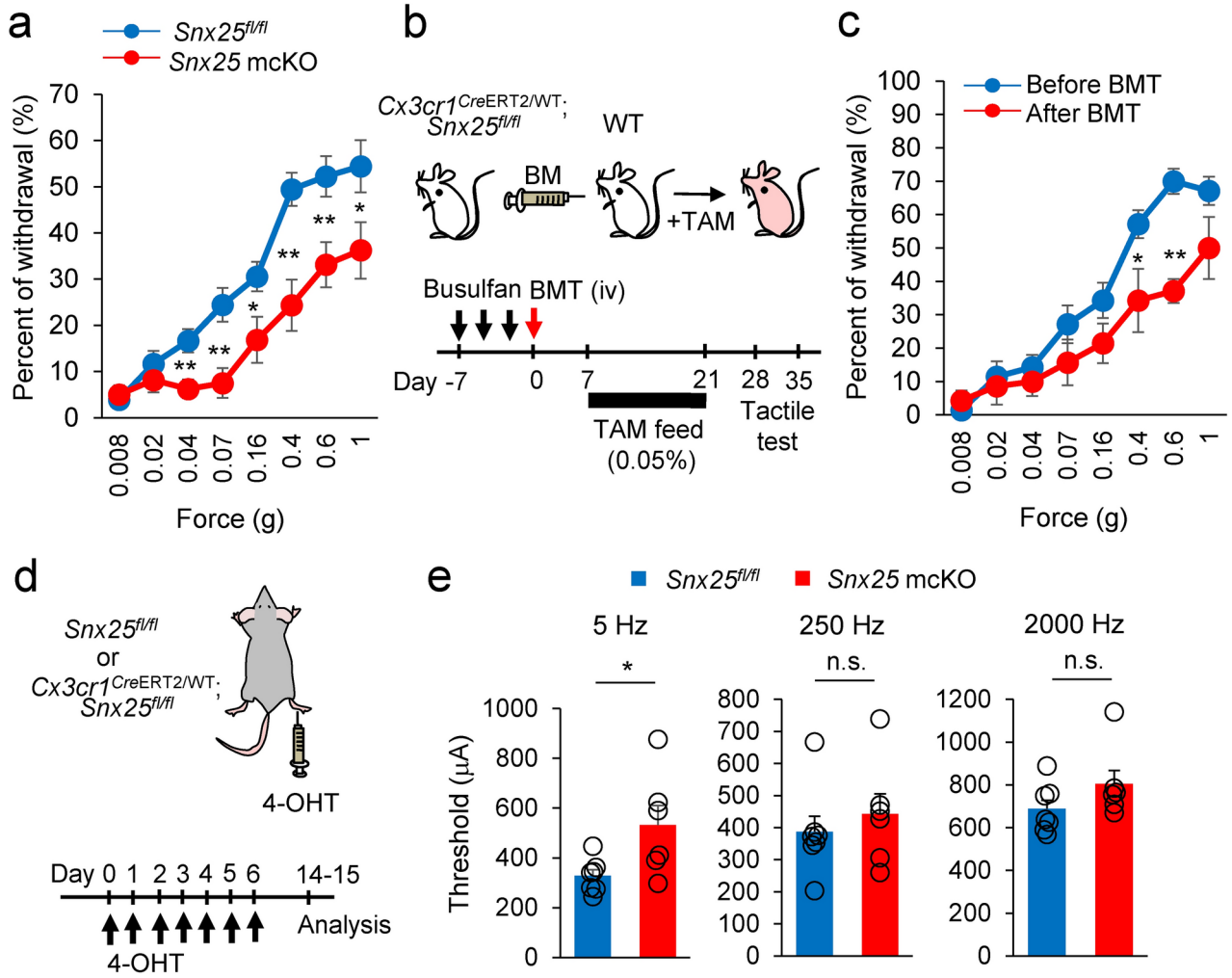

Fig. 2. *Snx25* mcKO yields a tactile-insensitive phenotype. (**a**) Fine tactile sensitivity was examined with von Frey filaments whose mechanical pressure ranged from 0.008 g to 1 g. The percentages of withdrawal (positive response) to innocuous low-pressure stimuli were plotted (*Snx25*$^{fl/fl}$ mice: n = 18; *Snx25* mcKO mice: n = 16). 0.04g; $p = 0.004$, 0.07g; $p = 0.002$, 0.16g; $p = 0.024$, 0.4g; $p = 0.0005$, 0.6g; $p = 0.006$, 1.0g; $p = 0.036$. (**b**) Schedules for generation of BM chimeric mice by transplanting *Snx25* mcKO BM into WT mice, and subsequent tactile test. (**c**) Tactile test in chimeric mice (*Snx25* mcKO BM → WT: n = 7, 35 days after BMT). 0.4g; $p = 0.048$, 0.6g; $p = 3.955e\text{-}05$. (**d**) Scheme depicting dermal injection of 4-OHT into hind paws of a *Cx3cr1*$^{CreERT2/WT}$; *Snx25*$^{fl/fl}$ mouse and experimental time course. To achieve gene recombination, we injected 4-OHT daily for 7 days and evaluated responses of sensory afferent fibers using transcutaneous sine wave stimuli at 8–9 days after the last injection. (**e**) Paw withdrawal thresholds in response to sine-wave electrical stimuli in *Snx25* mcKO mice. The current threshold represents the minimum intensity (μA) required to produce a paw withdrawal response with sine-wave electrical stimulation at 5, 250, and 2000 Hz (*Snx25*$^{fl/fl}$ mice: n = 7; *Snx25* mcKO mice: n = 6). 5Hz; $p = 0.033$, 250Hz; $p = 0.525$, 2000Hz; $p = 0.171$. The data are expressed as the mean ± S.E.M. $^{*}p < 0.05$, $^{**}p < 0.01$, n.s., not significant. Results are represented as mean ± SEM. Statistical analyses were performed using the Student's *t*-test.

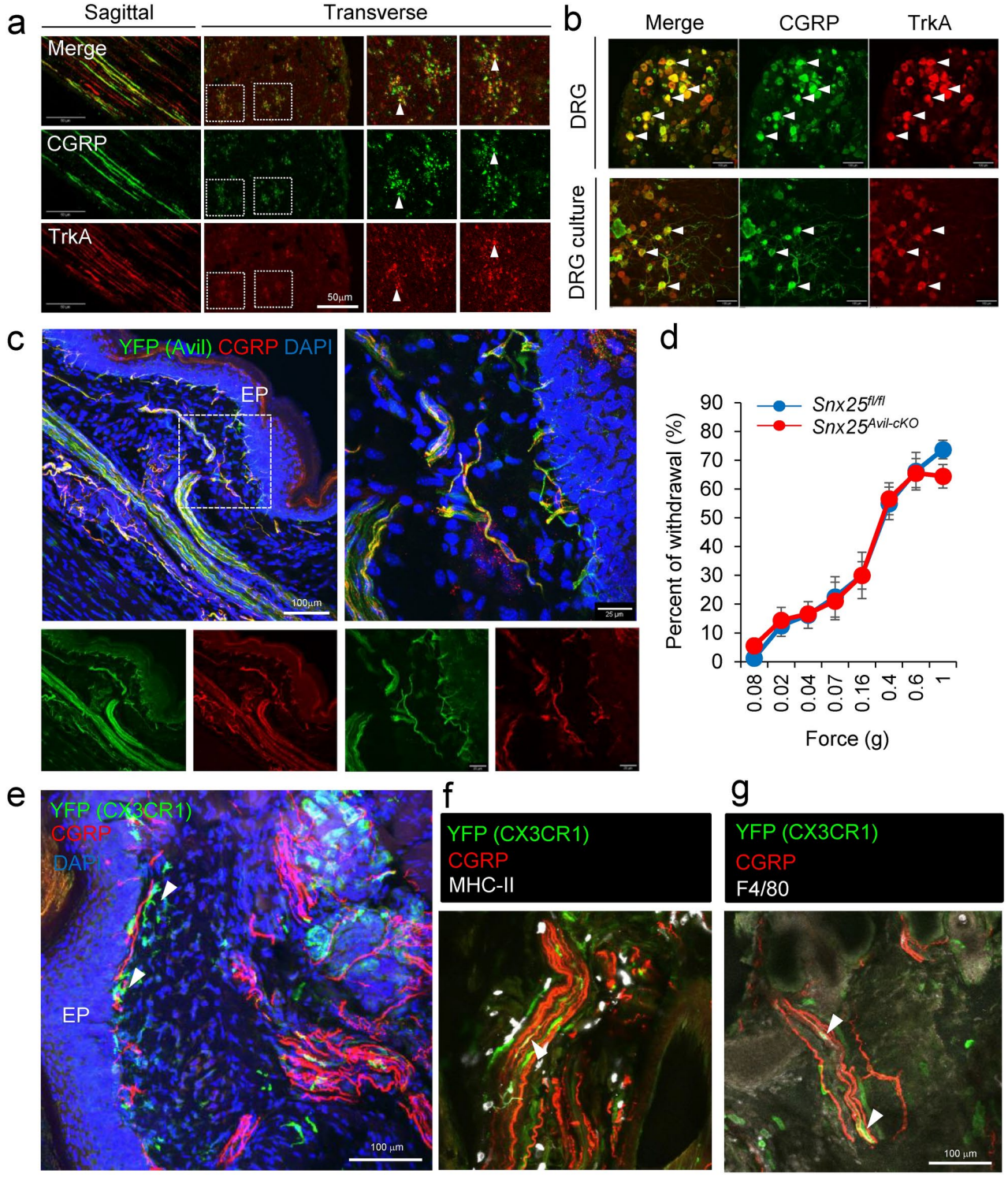

after transplantation, and we confirmed that the cells recombined during this period fully expressed *Cre* in peripheral blood (Supplementary Fig. 1a and b). In WT mice that received BM from *Snx25* mcKO; Ai32$^{Tg/+}$ mice (see Methods), Ai32$^{Tg/+}$-derived YFP expression was detected in 44% [6] of MHC-II + dermal macrophages in situ following oral TAM treatment (Supplementary Fig. 1c). Furthermore, we confirmed that SNX25 was knocked out in YFP-positive macrophages in a BMT experiment with *Snx25*$^{Cx3cr1\text{-}cKO}$; Ai32$^{Tg/+}$ mice [6]. Percent of withdrawal from innocuous stimuli to the paws decreased at day 28d and 35 after BMT in WT mice (Fig. 2c, Supplementary Fig. 1d, and Supplementary Fig. 2). BMT between the same genotypes (WT to WT or *Snx25* KO to *Snx25* KO) did not also affect thresholds in von Frey test [6]. We assume that similar results would be obtained with the tactile test. These observations indicate that SNX25 in BM-derived nerve-associated dermal macrophages, but not CX3CR1-positive microglia, contributes to tactile sensation.

The tactile behavior assays revealed differences in sensitivity between *Snx25* mcKO and control mice. We next examined the responses of sensory afferent fibers using transcutaneous electrical stimuli that can differentiate

◀**Fig. 3**. SNX25-expressing dermal macrophages are closely associated with CGRP-positive fibers. (**a**) Confocal images of the sciatic nerve of WT mice, stained with anti-CGRP and TrkA antibody. The left panels are a sagittal section and the right panels are a transverse section. Arrowheads denote CGRP$^+$ TrkA$^+$ nerves. (**b**) Confocal images of the DRG of WT mice, stained with anti-CGRP and TrkA antibody. The upper panels are DRGs and the lower panels are a primary DRG neurons. Arrowheads denote CGRP$^+$ TrkA$^+$ cells. (**c**) Confocal images of hind paw skin (naïve) stained for YFP (green) and CGRP (red) in TAM-treated *Avil*^{CreER}; Ai32 mice. EP, epidermis. (**d**) Fine tactile sensitivity was examined with von Frey filaments whose mechanical pressure ranged from 0.008 g to 1 g. The percentages of withdrawal from innocuous low-pressure stimuli were plotted (*Snx25*$^{fl/fl}$ mice: n = 8; *Snx25*$^{Avil\text{-}cKO}$ mice: n = 9). (**e**) Confocal images of hind paw skin (naïve) stained for YFP (green) and CGRP (red) in 4-OHT-treated *Cx3cr1*^{CreER}; *Snx25*$^{fl/fl}$; Ai32 mice. Arrowheads denote nerve-associated YFP$^+$ cells. EP, epidermis. (**f**) Confocal images of hind paw skin (naïve) stained for YFP (green), MHC-II (white), and CGRP (red) in 4-OHT-treated *Cx3cr1*^{CreER}; *Snx25*$^{fl/fl}$; Ai32 mice. Arrowheads denote nerve-associated YFP$^+$ MHC-II $^+$ cells. (**g**) Confocal images of hind paw skin (naïve) stained for YFP (green), F4/80 (white), and CGRP (red) in 4-OHT-treated *Cx3cr1*^{CreER}; *Snx25*$^{fl/fl}$; Ai32 mice. Arrowheads denote nerve-associated YFP$^+$ F4/80 $^+$ cells. Results are represented as mean ± SEM. Statistical analyses were performed using the Student's *t*-test (**d**).

frequencies specific to Aβ, Aδ, and C fibers. We injected the soluble TAM derivative 4-OH tamoxifen (4-OHT) for seven days (once a day) into the hind paw of *Cx3cr1*^{CreER}; *Snx25*$^{fl/fl}$ mice to knock out *Snx25* locally in dermal macrophages (Fig. 2d). Transcutaneous nerve stimulation was conducted with three sine wave pulses with frequencies of 5, 250, and 2000 Hz to activate C, Aδ, and Aβ fibers, respectively. As shown in Fig. 2e, the application of 5-Hz stimulus to the hind paw of *Snx25* mcKO mice yielded a significant increase in the paw withdrawal threshold compared to that of control mice at 8–9 days after the last injection (Fig. 2e). In contrast, the thresholds for the 250- and 2000-Hz stimulus responses were not changed in the *Snx25* mcKO mice compared with those in control mice (Fig. 2e). These data indicate that *Snx25* mcKO primarily affects C-fibers and reinforce the idea that SNX25 in CX3CR1$^+$ nerve-associated dermal macrophages regulates tactile perception of gentle mechanical force.

SNX25-expressing dermal macrophages are closely associated with CGRP- and TH-positive sensory fibers

Given that C-fibers probably contribute to the touch-insensitive phenotype of *Snx25*$^{+/-}$ mice and mcKO mice, we further characterized C-fibers with immunohistochemistry and immunocytochemistry. First, we hypothesized that reduced tactile sensation in *Snx25*$^{+/-}$ mice and *Snx25* mcKO mice were due to weakened activation of C-nociceptors and investigated the relation between C-nociceptors and dermal macrophages. CGRP is expressed by many peptidergic C-fiber nociceptors [18]. Immunohistochemical analysis in the sagittal and transverse sections of sciatic nerves revealed that some axons within the sciatic nerves are CGRP-positive (Fig. 3a). Immunohistochemical analysis of DRG revealed that some cell bodies are CGRP-positive and same results were obtained with primary cultures of DRG neuron (Fig. 3b). To investigate the localization of sensory nerves in the dermis, we crossed *Advillin* (*Avil*)^{CreERT2} mice with reporter mice harboring RCL-ChR2(H134R)/EYFP (Ai32) to generate *Avil* $^{CreER/WT}$; Ai32$^{Tg/+}$ mice, in which Advillin positive sensory nerves can be tracked by YFP expression. Nerve fibers run in bundles deep layer in the dermis, while many fine nerve fibers were localized in the dermis layer just beneath the epidermis (Fig. 3c). Next, to investigate the possible contribution of nerve-inherent SNX25, we conditionally deleted *Snx25* in the DRG by crossing *Snx25*$^{fl/fl}$ mice with *Avil*^{CreERT2} mice. The DRG-specific *Snx25* cKO mice had normal reactions to tactile stimuli (Fig. 3d). These results suggest that SNX25 in the DRG does not regulate tactile sensation under physiological conditions. Next, to determine the spatial relationship between SNX25-positive dermal macrophages and C-fibers, we crossed *Cx3cr1*$^{CreER/WT}$; *Snx25*$^{fl/fl}$ mice with Ai32 mice. YFP expression was detected in macrophages in the 4-OHT-injected hind paw skin of the *Snx25*$^{Cx3cr1\text{-}cKO}$; Ai32$^{Tg/+}$ mice, and YFP$^+$ CX3CR1$^+$ dermal macrophages were frequently found close to CGRP-positive fibers (arrowheads) that innervate the skin (Fig. 3e). YFP$^+$ CX3CR1$^+$ dermal macrophages also expressed MHC-II (Fig. 3f) and/or F4/80 (Fig. 3g), demonstrating that they were indeed macrophages. These results indicated that dermal macrophages associate with sensory C-fibers and that SNX25 in these macrophages (but not SNX25 in sensory neurons) regulates tactile sensitivity.

On the other hand, it is known that in addition to nociceptive neurons, C-fibers also contain C-LTMRs involved in touch. C-LTMRs, the slowest-conducting mechanoreceptor subtype, make up a large fraction of DRG neurons (~15–30%) [4,5]. In mice, a population of C-LTMRs can be identified based on its expression of TH, VGLUT3, and Fam19a4[5]. Indeed, immunohistochemical analysis in the sagittal and transverse sections of sciatic nerves revealed that some of the sciatic nerves are TH-positive (Fig. 4a). Immunohistochemical analysis of DRG revealed that some cell bodies are TH-positive and same results were obtained with primary cultures of DRG neuron (Fig. 4b). Although CGRP and TH appear to be partially co-expressed in the sciatic nerve fibers (Fig. 4c, arrowhead), peripheral nerve fibers run in Remak bundles and single axons cannot be identified. Therefore, we examined CGRP and TH expression in DRG and primary cultures of DRG neuron and found that some neurons were double positive for CGRP and TH (Fig. 4d, arrowheads). To investigate the relation between TH-positive C-LTMRs and CX3CR1-positive macrophages, we again used *Snx25*$^{Cx3cr1\text{-}cKO}$; Ai32$^{Tg/+}$ mice. Immunohistochemical data showed that YFP-positive macrophages associated with TH-positive nerves (arrowhead) in the dermis (Fig. 4e and Supplementary Fig. 3a). These nerve-associated YFP cells were also MHC-II- (Fig. 4f and Supplementary Fig. 3b, arrowheads) and/or F4/80-positive macrophages (Fig. 4g, arrowheads). These results, together with the electrical stimulation-induced paw withdrawal test, indicated that

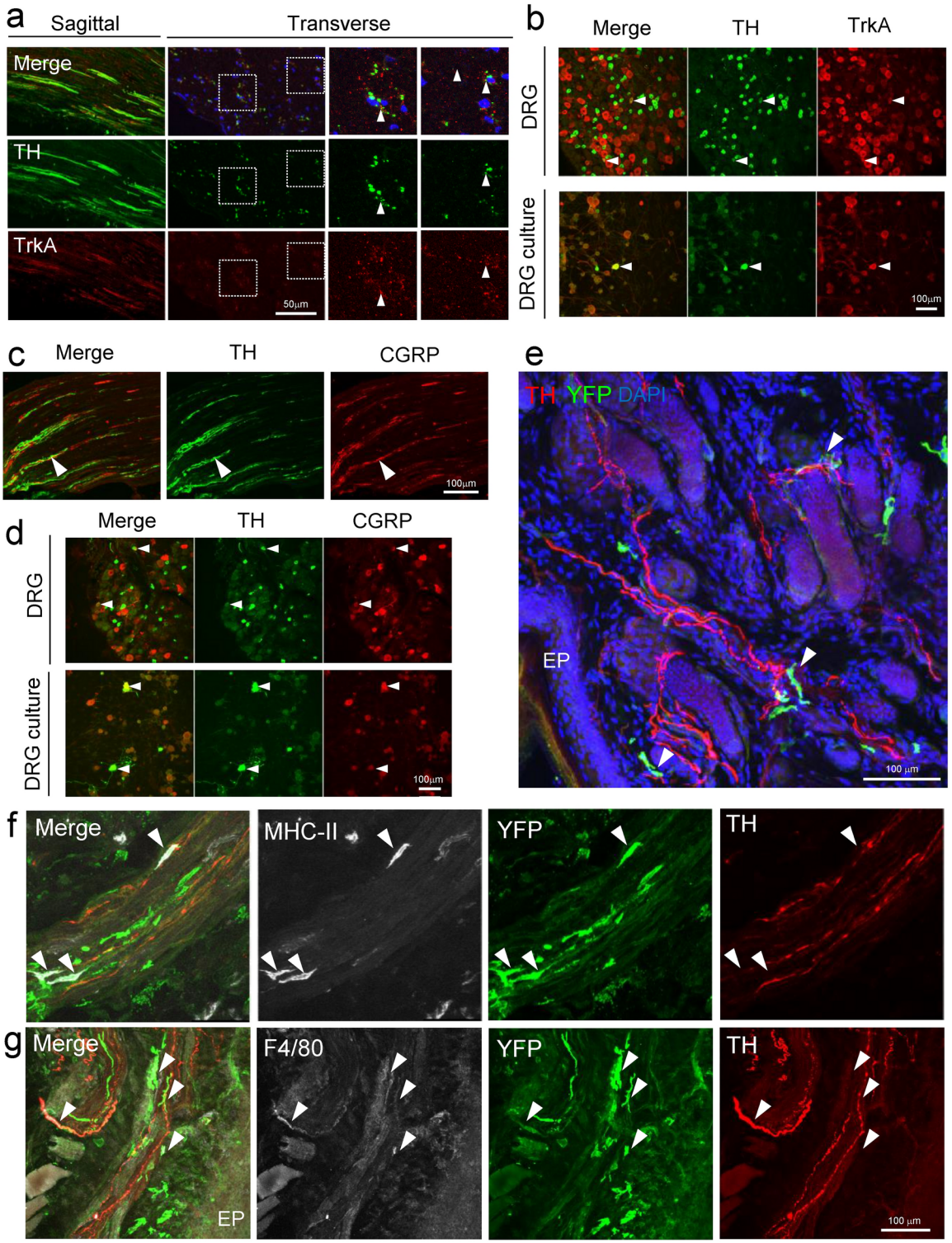

dermal macrophages associate with sensory C-fibers and that SNX25 in these macrophages regulates tactile sensitivity. Immunostaining data in the skin of TH shows that macrophages are often associated with C-LTMR fibers (although in some CGRP and TH colocalize) in addition to C-nociceptors, and it remains possible that CX3CR1-positive nerve-associated macrophages have some effect on tactile perception via SNX25 signaling.

NGF and SNX25 are expressed in dermal macrophages

Our previous study demonstrated that SNX25 in dermal macrophages regulates NGF expression and that lowering NGF levels yielded mice with the pain-insensitive phenotype [6]. To address the question of whether dermal macrophages are necessary for tissue NGF content and tactile sensation, we depleted dermal macrophages by intradermal injection (i.d.) of clodronate liposomes (Clo lipo), a well-characterized macrophage killer, twice into one side of the hind paw (Fig. 5a). Immunohistochemistry revealed that the numbers of CD206-positive

Fig. 4. SNX25-expressing dermal macrophages are closely associated with TH-positive fibers. (**a**) Confocal images of the sciatic nerve of WT mice, stained with anti-TH and TrkA antibody. The left panels are a sagittal section and the right panels are a transverse section. Arrowheads denote TH^+ $TrkA^+$ nerves. (**b**) Confocal images of the DRG of WT mice, stained with anti-TH and TrkA antibody. The upper panels are DRGs and the lower panels are a primary DRG neurons. Arrowheads denote TH^+ $TrkA^+$ cells. (**c**) Confocal images of the sciatic nerve of WT mice, stained with anti-CGRP and TH antibody. Arrowheads denote $CGRP^+$ TH^+ cells. (**d**) Confocal images of the DRG of WT mice and primary DRG neurons, stained with anti-CGRP and TH antibody. Arrowheads denote $CGRP^+$ TH^+ cells. (**e**) Confocal images of hind paw skin (naïve) stained for YFP (green) and TH (red) in 4-OHT-treated *Cx3cr1*^{CreER}; *Snx25*$^{fl/fl}$; Ai32 mice. Arrowheads denote nerve-associated YFP^+ cells. EP, epidermis. (**f**) Confocal images of hind paw skin (naïve) stained for YFP (green), MHC-II (white), and TH (red) in 4-OHT-treated *Cx3cr1*^{CreER}; *Snx25*$^{fl/fl}$; Ai32 mice. Arrowheads denote nerve-associated YFP^+ MHC-II^+ cells. (**g**) Confocal images of hind paw skin (naïve) stained for YFP (green), F4/80 (white), and TH (red) in 4-OHT-treated *Cx3cr1*^{CreER}; *Snx25*$^{fl/fl}$; Ai32 mice. EP, epidermis. Arrowheads denote nerve-associated YFP^+ $F4/80^+$ cells.

macrophages had decreased at 3 days after the second Clo lipo injection relative to the control liposome (Con lipo)-injected skin (Supplementary Fig. 4a). We also examined the Clo lipo-induced depletion of dermal macrophages by fluorescence-activated cell sorting (FACS). The majority of dermal macrophages defined by the expression of $Ly6c^{low}$ $CD11c^{low}$ MHC-II^{high} population were reduced in hind paw skin (Supplementary Fig. 4b). We also confirmed by Western blotting that the population of CD206-positive dermal macrophages was decreased after the Clo lipo injection relative to the Con lipo-injected skin (Supplementary Fig. 4c). Further Western blot analyses revealed that NGF and SNX25 expression levels were lower in the Clo lipo-injected area than in the Con lipo-injected area (Supplementary Fig. 4c). Taken together, these findings indicate that NGF and SNX25 are expressed mainly in dermal macrophages. To investigate the roles of dermal macrophages in tactile sensation, we examined the responses to low-pressure punctate stimuli in the Clo lipo-injected mice and found that they were weaker (Fig. 5b and Supplementary Fig. 4d), suggesting that dermal macrophages are involved in innocuous tactile sensitivity.

There is a close relationship between mechanical stimulation and tissue NGF production [19]. To test the hypothesis that mechanical stimuli cause NGF synthesis in macrophages, BMDMs were stretched by 12.5% in a stretch chamber and the time course of NGF expression was examined (Fig. 5c). As expected, NGF expression in response to the mechanical stimulus tended to be higher than in the control group, but there was no significant difference (Fig. 5d and e). These results suggest that mechanical stimuli to macrophages contribute to a transient increase in NGF expression.

NGF signaling is required for tactile sensation

We focused on NGF as a causative factor for the tactile-insensitive behavior of *Snx25*$^{+/-}$ and *Snx25* mcKO mice, because mechanosensory factors including *Trpv2*, *Trpc1*, and *Scn10a*, whose expression was reduced in the *Snx25*$^{+/-}$ DRGs (Fig. 1b), are all transcriptionally regulated by peripheral tissue-derived and retrogradely transported NGF [10]. If NGF is responsible, injection of NGF (Fig. 6a) should render tactile perception more sensitive in both WT mice and *Snx25* mcKO mice. Indeed, NGF receptor TrkA was expressed CGRP-positive (Fig. 3a, b) and TH-positive C-fibers (Fig. 4a, b). TrkA is expressed in C-nociceptors, and it has been shown that TrkA is also present in the population that can be classified as C-LTMR [20]. These reports are consistent with our results. NGF (100 ng) was injected subcutaneously into the plantar surface of the right hind paw of WT mice and we then examined tactile sensation. Tactile sensitivity was increased at 24 h after intradermal injection of NGF (Fig. 6b), compared with PBS (Veh) injection. Prior to the increase in tactile sensitivity, the expression of mechanosensory factors (*Trpv1*, *Trpa1*, and *Trpc1*) in the DRG was also found to increase at 20 h after intradermal injection of NGF (Fig. 6c). These changes in gene expression were not observed at 10 h or 48 h after NGF injection (Supplementary Fig. 5). Injection of NGF into the skin likely contributed to a transient increase in mechanosensory gene expression in the DRG. Next, we investigated whether the dull phenotype of tactile sensitivity was rescued by intradermal injection of NGF in either the *Snx25*$^{+/-}$ or *Snx25* mcKO mice. *Snx25*$^{+/-}$ mice (Fig. 7a-b and Supplementary Fig. 6a) as well as *Snx25* mcKO mice (Fig. 7c-d) became sensitive to innocuous stimuli 24 h after NGF injection and were comparable to WT and *Snx25*$^{fl/fl}$ mice, respectively. Tactile sensitivity was also increased at 48 h postinjection, but the effect of NGF was slightly weaker than at 24 h (Supplementary Fig. 6b-c). These results suggest that NGF directly causes tactile sensitivity and that NGF level is modulated by SNX25 signaling.

Discussion

The functional anatomy[21] and neuro-immune interactions[22] of the peripheral sensory system have been elucidated at remarkable speed in recent years. However, the whole picture of tactile sensitivity mechanisms still remains unclear. In the present study, we have identified *Snx25* as a tactile sensitivity-modulating gene. Both *Snx25*$^{+/-}$ mice and *Snx25* mcKO mice displayed reduced light touch responses under normal conditions.

Recent progress in gene cataloging techniques such as single-cell RNA sequencing has broadened our knowledge of tissue macrophages. Chakarov et al. characterized two independent populations of lung interstitial macrophages exhibiting distinct gene expression profiles and phenotypes: $Lyve1^{lo}$ MHC-II^{hi} $CX3CR1^{hi}$ macrophages were associated with nerves, whereas $Lyve1^{hi}$ MHC-II^{lo} $CX3CR1^{lo}$ macrophages were preferentially located around blood vessels[13]. These macrophages were in part derived from bone marrow, consistent with fate-mapping studies[16,17]. We crossed *Cx3cr1*$^{CreERT2/WT}$ mice with the reporter line RCL-ChR2(H134R)/EYFP (Ai32),

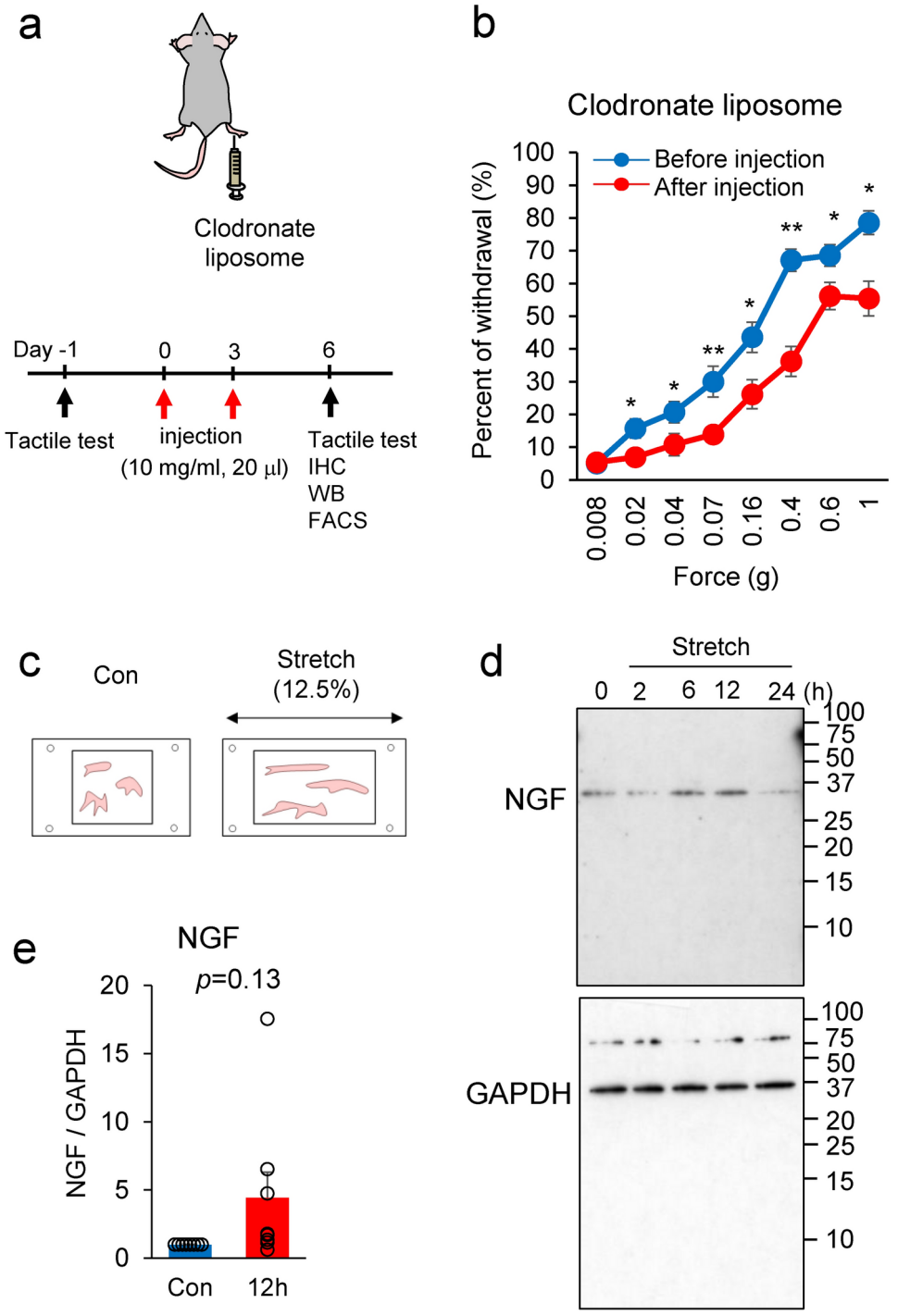

Fig. 5. NGF and SNX25 are expressed in dermal macrophages. **(a)** Scheme depicting dermal injection of clodronate liposome into the right hind paw and experimental schedule. (**b**) Fine tactile sensitivity was examined with von Frey filaments whose mechanical pressure ranged from 0.008 g to 1 g, in uninjected WT mice and in WT mice at 24 h after Clo lipo injection (n = 14). 0.02g; $p = 0.023$, 0.04g; $p = 0.046$, 0.07g; $p = 0.005$, 0.16g; $p = 0.013$, 0.4g; $p = 1.4e\text{-}05$, 0.6g; $p = 0.030$, 1.0g; $p = 0.001$. **(c)** Scheme depicting stretch of BMDMs. (**d**) Semi-quantitative analyses of NGF level in mechanically stretched BMDMs. BMDMs were exposed to mechanical stretch over 24 h. Mechanical stretch to 12.5% increased NGF protein expression in a time-dependent manner. (**e**) Semi-quantitative analyses of the immunoblots at 12 h (Con, n = 8; 12 h, n = 8). $p = 0.13$. The data are expressed as the mean ± S.E.M. $^{*}p < 0.05$, $^{**}p < 0.01$. Results are represented as mean ± SEM. Statistical analyses were performed using the Student's *t*-test (**b**).

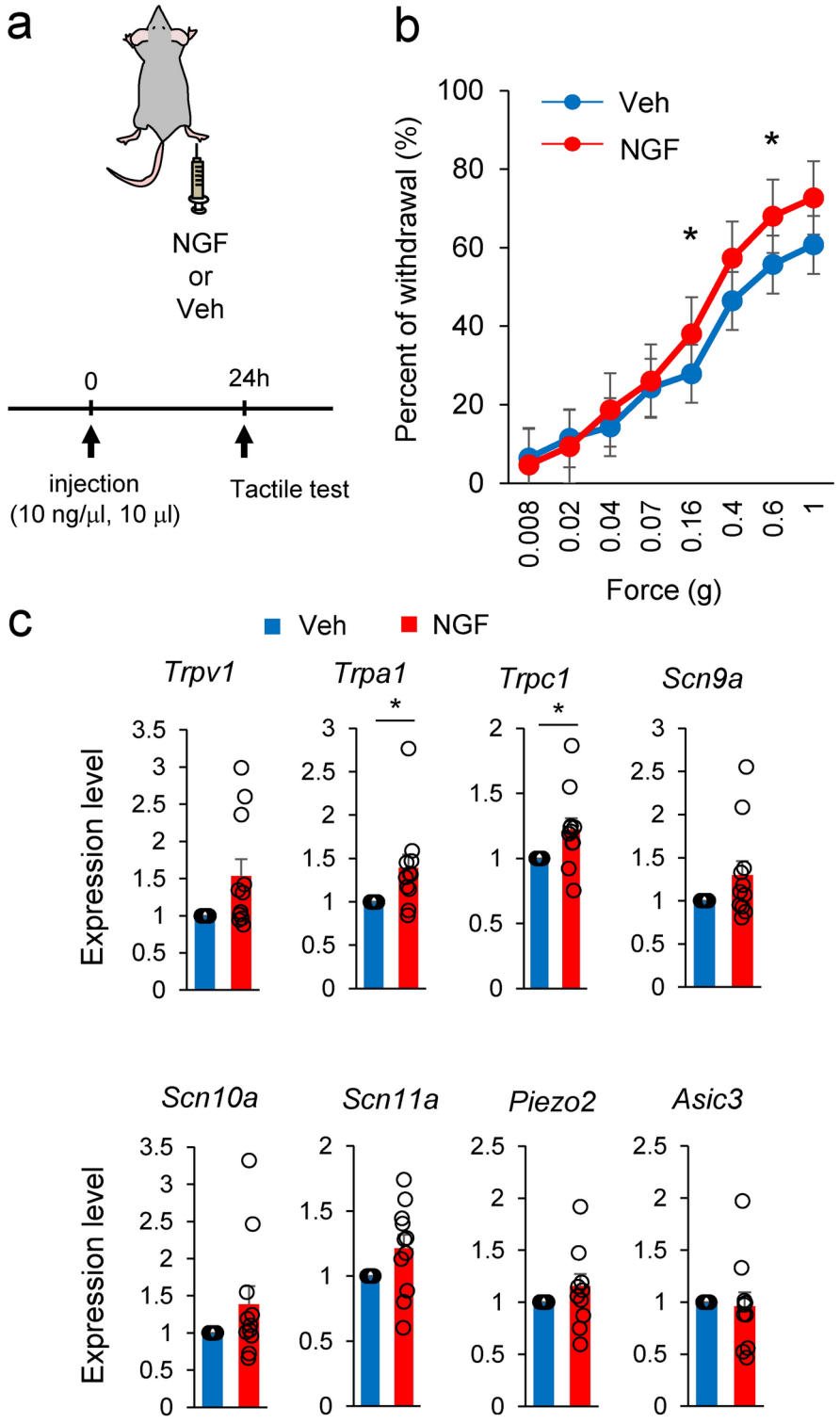

Fig. 6. NGF signaling is required for tactile sensation. **(a)** Scheme depicting dermal injection of NGF or PBS (Veh) into the right hind paw and experimental schedule. (**b**) Fine tactile sensitivity was examined with von Frey filaments whose mechanical pressure ranged from 0.008 g to 1 g, in NGF-injected mice and PBS-injected mice. 0.16g; $p = 0.048$, 0.6g; $p = 0.029$. (**c**) mRNA expression levels for mechanosensory factors in DRG of mice at 20 h after NGF or PBS injection (Veh: n = 14; NGF: n = 15). *Trpv1*; $p = 0.054$, *Trpa1*; $p = 0.035$, *Trpc1*; $p = 0.028$.*$p < 0.05$. Results are represented as mean ± SEM. Statistical analyses were performed using the Student's *t*-test (**b**) or Welch's *t*-test (**c**).

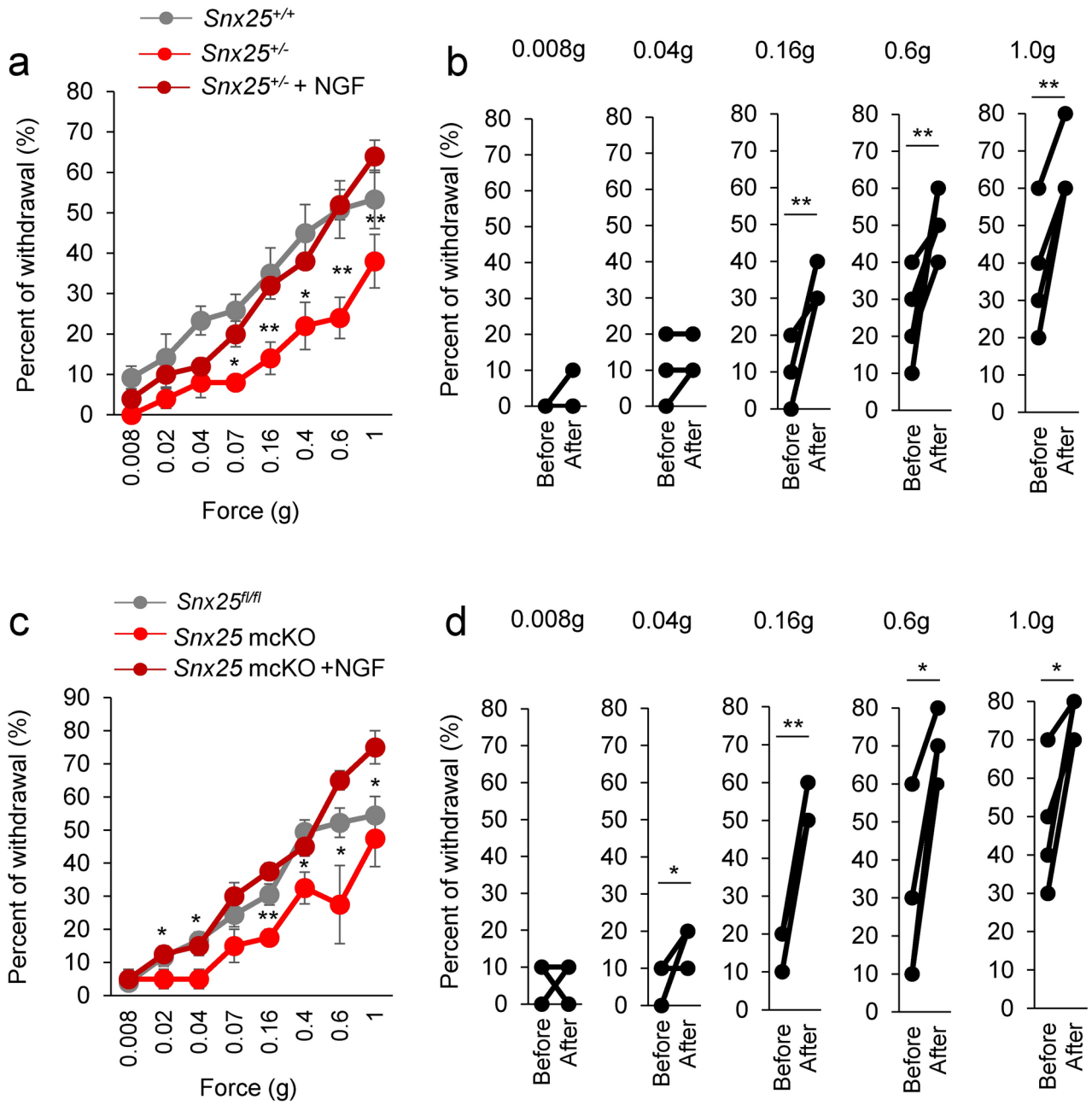

Fig. 7. Dull phenotype of tactile sensitivity is rescued by intradermal injection of NGF. (**a**) Fine tactile sensitivity was examined with von Frey filaments whose mechanical pressure ranged from 0.008 g to 1 g, in *Snx25*$^{+/-}$ mice and in *Snx25*$^{+/-}$ mice at 24 h after NGF injection (n = 5). 0.07g; $p = 0.012$, 0.16g; $p = 0.004$, 0.4g; $p = 0.032$, 0.6g; $p = 0.002$, 1.0g; $p = 0.001$. (**b**) Changes of percent of withdrawal on the side injected with NGF of each *Snx25*$^{+/-}$ mouse (n = 5). 0.16g; $p = 0.004$, 0.6g; $p = 0.002$, 1.0g; $p = 0.001$. (**c**) Fine tactile sensitivity was examined with von Frey filaments as above, in *Snx25* mcKO mice and in *Snx25* mcKO mice at 24 h after NGF injection (n = 4). 0.02g; $p = 0.017$, 0.04g; $p = 0.017$, 0.16g; $p = 6.14\text{e-}05$, 0.4g; $p = 0.001$, 0.6g; $p = 0.015$, 1.0g; $p = 0.022$. (**d**) Changes of percent of withdrawal on the side injected with NGF of each *Snx25* mcKO mouse (n = 4). 0.04g; $p = 0.017$, 0.16g; $p = 6.14\text{e-}05$, 0.6g; $p = 0.015$, 1.0g; $p = 0.022$.*$p < 0.05$, **$p < 0.01$. Results are represented as mean ± SEM. Statistical analyses were performed using the Student's *t*-test (*Snx25*$^{+/-}$ vs *Snx25*$^{+/-}$ + NGF, or *Snx25* mcKO vs *Snx25* mcKO + NGF).

and YFP-positive dermal macrophages were frequently found close to CGRP-positive C-nociceptors in just beneath the epidermis in addition to nerves that run as bundles in deep layer. Our data indicated that the reduced tactile sensation in *Snx25*$^{+/-}$ mice and *Snx25* mcKO mice was due to weakened activation of C-nociceptors. This finding is consistent with a previous report that CX3CR1^{hi} macrophages colocalize with peripheral nerves, which contributes to the surveillance and regeneration of local nerves in the dermis[16]. On the other hand, TH-positive C-LTMRs also innervate the skin. It has been reported that these neurons involved in apparently opposing

sensations of pleasant touch and hypersensitivity during chronic pain[12,23], although their detail function remain unknown. Since dermal macrophages also associate with TH-positive nerves and these nerves also express the NGF receptor TrkA, it remains possible that macrophages associated with C-LTMRs may also be involved in tactile sensation via NGF-TrkA signaling. As shown in Fig. 2e, the application of 5-Hz stimulus to the hind paw of *Snx25* mcKO mice yielded a significant increase in the paw withdrawal threshold compared to that of control mice (Fig. 2e). These data indicate that *Snx25* mcKO primarily affects C-fibers and reinforce the idea that SNX25 in CX3CR1 + nerve-associated dermal macrophages regulate tactile perception of gentle mechanical force. However, it has been also reported that the key feature of C-LTMRs is their high discharge frequency (> 100 Hz) upon a preferred stroking velocity [23,24], therefore macrophages that associate with C-LTMR may not be involved in the regulation of tactile sensation via SNX25-NGF-TrkA. Further characterization of dermal macrophages associated with C-LTMR and investigation of its function might provide new insights into crucial role under physiological conditions.

NGF production by these dermal macrophages likely contributes to the regeneration of local nerves in addition to the maintenance of pain sensibility. Macrophages are known to adhere to the cell matrix at a specialized structure, the podosome[25]. Podosomes confer on dermal macrophages the ability to sense mechanical stress and deformation of tissues [25,26]. It is interesting to speculate that the mechano-sensing ability of dermal macrophages is linked to NGF production and thereby regulates mechanical tactile sensitivity. In line with this speculation, NGF tended to be upregulated in response to sustained mechanical stretch in cultured bone marrow-derived macrophages. In the present study, we continuously stretched macrophages for 12 h in vitro to recapitulate the in vivo situation (Fig. 5c-e). Considering that dermal macrophages are repeatedly stretched and relaxed, in vitro experiments that mimic these environments may be necessary in future studies. Taking all these observations together, local inflammation including mechanical stress stimulate dermal macrophages, and the macrophages then optimize the NGF concentration for neurons to respond to stimuli via SNX25. We propose that the tissue (dermis in the present study) content of NGF is continuously controlled at least in part by macrophages through SNX25–Nrf2–NGF signaling. In this hypothesis, the tissue levels of NGF parallels the mechanical tactile and pain sensitivities: the higher the NGF level, the more sensitive the animal or tissue is, and vice versa. NGF is also produced by noninflammatory cells, such as keratinocytes and endothelial cells[27], in addition to other inflammatory cells, such as fibroblasts. Thus, further experiments are needed to determine the entire cellular and molecular mechanism controlling peripheral NGF level and tactile perception.

Methods

Animals

Snx25 constitutive KO (*Snx25*$^{+/-}$) mice (B6/N-*Snx25*$^{tm1a/Nju}$, Nanjing BioMedical Research Institute of Nanjing University (NBRI); strain name, B6/N-*Snx25*$^{tm1a/Nju}$, strain number T001400) were obtained from NBRI. *Snx25* cKO mice were generated by first crossing our *Snx25* LacZ/ + mice with CAG-Flpo mice (B6. Cg-Tg(CAG-FLPo)/1Osb), which were a gift from M. Ikawa (Osaka University), in order to excise the LacZ cassette framed by *Frt* sites and obtain an allele with floxed exon 4 (*Snx25*$^{fl/fl}$ mice)[28]. We crossed *Cx3cr1*^{CreERT2} mice (B6.129P2(C)-*Cx3cr1*$^{tm2.1(Cre/ERT2)Jung/J}$) (Jackson Laboratory, Stock No. 020940) with *Snx25*$^{fl/fl}$ mice to obtain *Cx3cr1*$^{CreERT2/WT}$; *Snx25*$^{fl/fl}$ mice (*Cx3cr1*^{CreER}; *Snx25*$^{fl/fl}$). We crossed *Cx3cr1*$^{CreERT2/WT}$; *Snx25*$^{fl/fl}$ mice with reporter mice RCL-ChR2(H134R)/EYFP (Ai32 mice, Jackson Laboratory, Stock No. 012569) to obtain *Cx3cr1*$^{CreERT2/WT}$; *Snx25*$^{fl/fl}$; Ai32$^{/+}$ mice (*Cx3cr1*^{CreER}; *Snx25*$^{fl/fl}$; Ai32). We crossed *Advillin*-cre mice (B6.Cg-Tg(*Avil-Cre*/ERT2)AJwo/J) (Jackson Laboratory, Stock No. 032027) with *Snx25*$^{fl/fl}$ mice to obtain *Avil*$^{CreERT2/WT}$; *Snx25*$^{fl/fl}$ mice. We crossed *Advillin-Cre* mice with reporter mice RCL-ChR2(H134R)/EYFP (Ai32 mice) to obtain *Avil*$^{CreERT2/WT}$; Ai32$^{/+}$ mice (*Avil*^{CreER}; Ai32). All mice were housed in standard cages under a 12-h light/dark cycle and temperature-controlled conditions. All protocols for animal experiments were approved by the Animal Care Committee of Nara Medical University. All animal experiments are conducted in accordance with the policies established in the NIH Guide for the Care and Use of Laboratory Animals. This study was also carried out in compliance with the ARRIVE guidelines (https://arriveguidelines.org/). Euthanasia was performed by blood release under deep anesthesia (medetomidine, midazolam, and butorphanol), by perfusion fixation, or by cervical dislocation.

Behavioral test

To assess sensitivity to a weak tactile stimulus, mice were acclimatized for at least 15 min in individual clear acrylic cubicles (10 × 10 × 10 cm) placed on top of an elevated wire mesh. Calibrated von Frey's filaments (Muromachi kikai, 0.008–1 *g*) were used to stimulate the plantar surface of the hind paws. Withdrawal immediately after the 1 s stimulus was considered as a positive response. The plantar surface was stimulated 10 times with each filament and the number of positive responses was measured. For the tactile test after NGF (N-240, Alomone Labs) injection, 100 ng NGF (10 µl) was injected subcutaneously into the plantar surface of the right hind paw.

Reagents

For tamoxifen (TAM) treatment, we employed oral administration. TAM (T5648, Sigma-Aldrich) was mixed with powdered chow (0.5 mg/g normal chow). This oral administration method is convenient for continuous administration and results in efficient induction of recombination while minimizing stress on the mice[15]. For depletion of macrophages in hind paw skin, we used clodronate liposomes (MKV300, Cosmo Bio).

Clodronate liposome treatment

Twenty microliters of 10 mg/ml clodronate liposomes or control liposomes (MKV300) were subcutaneously injected into the right side of the hind paw skin on days 0 and 3. Three days after the second injection, a tactile test was performed.

4-OHT treatment

For depletion of SNX25 in dermal macrophages, we administered 4-OHT (40 ng/μl, 10 μl) by intradermal injection daily for seven days into *Cx3cr1*^{CreER}; *Snx25*$^{fl/fl}$ mice or *Cx3cr1*^{CreER}; *Snx25*$^{fl/fl}$; Ai32 mice. Vehicle was injected into the contralateral side of the same animal. At 8 days after the last injection, a tactile test was performed.

Immunohistochemistry

Mice were anesthetized and perfused transcardially with saline followed by 4% paraformaldehyde (PFA, 09,154–85, Nacalai Tesque) in 0.1 M phosphate buffer (pH 7.4) (PB). Skin, DRG, sciatic nerve, and spinal cord were removed, postfixed overnight in the same fixative, and then immersed in 30% sucrose in PB overnight. Next, the tissues were frozen in powdered dry ice, embedded in Tissue-Tek OCT compound (4583, Sakura Finetek), and stored at -80 °C prior to sectioning. Eighteen-micrometer-thick sections were immersed in PBS containing 5% bovine serum albumin and 0.3% Triton X-100 for 1 h. Antibodies against rabbit anti-CGRP (1:2000, C8198, Sigma), goat anti-CGRP (1:500, ab36001, abcam), rabbit anti-TH (1:500, 657,012, Calbiochem), rabbit anti-TrkA (1:150, ab76291, Abcam), goat anti-TrkA (1:100, AF1056, R&D Systems), rat anti-MHC-II (1:500, NBP1-43,312, Novus Biologicals), rat anti-F4/80 (1:500, NB600-404, Novus Biologicals), guinea pig anti-GFP (1:500, 132,004, Synaptic Systems), rat anti-GFP (1:5000, 04404–84, Nacalai Tesque), and rabbit anti-GFP (1:5000, A6455, Thermo Fisher Scientific) were applied overnight at 4 °C. Alexa Fluor 488-, 594- and 647-conjugated IgG (1:1000, Life Technologies) were used as secondary antibodies. Images were captured using a confocal laser scanning microscope (C2, Nikon).

qRT-PCR

Total RNA of cells or tissues was extracted using a NucleoSpin RNA Kit (740,955, Takara Bio). Total RNA extracts were reverse-transcribed using random primers and a QuantiTect Reverse Transcription kit (205,311, Qiagen), according to the manufacturer's instructions. Real-time PCR was performed using a Thermal Cycler Dice Real Time System (Takara Bio), with THUNDERBIRD SYBR qPCR Mix (QPS-201, Toyobo). PCR primers used in this study were as follows (all 5′→3′): *Asic3* sense primer, TAAGACCACCCTGGATGAGC, and *Asic3* antisense primer, GTAGGCAGCATGTTCAGCAG; *β-actin* sense primer, AGCCATGTACGTAGCCATCC; *β-actin* antisense primer, CTCTCAGCTGTGGTGGTGAA; *Ngf* sense primer, 5'-TCAGCATTCCCTTGACA CAG-3'; *Ngf* antisense primer, 5'-GTCTGAAGAGGTGGGTGGAG-3'; *Piezo1* sense primer, CCCTGTTACG CTTCAATGCT; and *Piezo1* antisense primer, GCTACCGTTTTGTCCCAGAA; *Piezo2* sense primer, GAACC AACCAAAGCAACGAT; and *Piezo2* antisense primer, AGGCACAAATACCCTGATGC; *Scn9a* sense primer, AAGGTCCCAAGCCCAGTAGT; *Scn9a* antisense primer, AGGACTGAAGGGAGACAGCA; *Scn10a* sense primer, GCCTCAGTTGGACTTGAAGG; *Scn10a*, antisense primer, AGGGACTGAAGAGCCACAGA; *Scn11a* sense primer, TGATCTTCCCAGACGAGAGG; and *Scn11a* antisense primer, ATAAGGTCAGGGGGAACGT C; *Trpv1* sense primer, CCCTCCAGACAGAGACCCTA; and *Trpv1* antisense primer, GACAACAGAGCTGAC GGTGA; *Trpa1* sense primer, CATGGACTGCTCCAAGGAAT; and *Trpa1* antisense primer, GCACTTCACAC GAAGAACCA; *Trpv2* sense primer, GCAGTGCTGAGGTGAACAAA; and *Trpv2* antisense primer, CCACACT GAAGAGTCGGTCA; *Trpc1* sense primer, ATGTGCGAGAGGTGAAGGAG; and *Trpc1* antisense primer, ACA GCATTTCTCCCAAGCAC; *Trek1* sense primer, GCTGCTCAGAACTCCAAACC; and *Trek1* antisense primer, TGGGCTATGAAGGTCTGCTT. Gene expression was quantified by the ΔΔCt method. Briefly, the relative concentration of the target gene and the reference gene (β-actin) was measured, and the relative concentration of the unknown concentration sample with respect to the reference gene was comparatively quantified. The signal value was denoted as a fold change corrected by the signal value of control (*Snx25*$^{+/+}$, vehicle).

Western blotting

Tissue samples were lysed with 10 mM Tris, pH 7.4, containing 150 mM NaCl, 5 mM EDTA, 1% Triton X-100, 1% deoxycholic acid, and 0.1% sodium dodecyl sulfate (SDS). The homogenate was centrifuged at 20,600 g for 5 min, and the supernatant was stored at -20 °C. Protein concentration was measured using a bicinchoninic acid protein assay kit (23,225, Thermo Fisher Scientific). Equal amounts (5 μg) of protein per lane were electrophoresed on SDS–polyacrylamide gels, and then transferred to a polyvinylidene difluoride membrane. The blots were probed with rabbit anti-NGF (1:200, sc-548, Santa Cruz Biotechnology), rabbit anti-SNX25 (1:100, 13,294–1-AP, Proteintech), goat anti-CD206 (1:1000, AF2535, R&D Systems) and rabbit anti-GAPDH (1:2000, ABS16, Merck Millipore) antibodies. Immunoblot analysis was performed with horseradish peroxidase-conjugated anti-rabbit and anti-goat IgG using enhanced chemiluminescence Western blotting detection reagents (297–72,403 or 290–69,904, Wako). Data were acquired in arbitrary densitometric units using ImageJ software (ImageJ ver. 1.54f., https://imagej.net/ij/index.html).

Primary DRG neurons

DRGs from WT mice were quickly collected in DMEM/F12 medium and incubated for 90 min at 37 °C in a 0.2% collagenase solution. After dissociation, DRGs were transferred to a tube containing DMEM/F12 supplemented with 10% fetal bovine serum (FBS), 1% penicillin/streptomycin solution. Ganglia were gently triturated using pipettes. After centrifugation, cells were resuspended in DMEM/F12 supplemented as above and plated on poly-L-lysine-coated culture dishes. Neurons were kept at 37 °C in 5% CO_2 and the medium was changed to DMEM/F12 with B27 supplement 8 h after plating.

Mechanical stretch of BMDMs

For the mechanical stretch experiment, BMDMs were seeded in a stretch chamber (STB-CH-04, STREX, Osaka, Japan) coated with 0.05 mg/ml fibronectin (Millipore, #FC010) and exposed to stretch up to 12.5%. Unstretched control BMDMs were treated equally but without application of mechanical stretch.

Bone marrow (BM) transplantation

BM recipients were male 8-week-old WT mice. Mice were intraperitoneally injected with the chemotherapeutic agent busulfan (30 μg/g body weight; B2635, Sigma-Aldrich) in a 1:4 solution of dimethyl sulfoxide and PBS at 7, 5, and 3 days prior to BM transfer. All mice were treated with antibiotics (trimethoprim (35,039, Nacalai Tesque) and sulfamethoxazole (S7507, Sigma)) for 14 days after busulfan treatment. BM-derived cells were obtained from the femur and tibia of 5-week-old *Cx3cr1*^{CreER}; *Snx25*$^{fl/fl}$ mice and resuspended in PBS with 2% FBS. BM-derived cells (1×10^6) were transferred to recipient mice by tail vein injection.

Fluorescence-activated cell sorting (FACS)

For the analysis of the myeloid population in the skin, cells were obtained from hind paw skin from three mice using a Multi Tissue Dissociation Kit 1 (130–110-201, Miltenyi Biotec) with a gentleMACS dissociator (Miltenyi Biotec) according to the manufacturer's instruction. The hind paw skin was minced by razor blade, and then subjected to enzymatic digestion at 37 °C, for 2 h with rotation. During the enzymatic digestion, cells were dispersed by the programs (h_tumor_01, h_tumor_02, and h_tumor_03) of gentleMACS. Debris was removed by a 70-μm cell strainer. The cells were stained with various combinations of the following mAbs: Biotin-anti-CD19 (115,504, BioLegend), Biotin-anti-NK1.1 (108,704, BioLegend), APC anti-MHC-II (107,613, BioLegend), FITC–anti-CD11c (107,305, BioLegend), PE-anti-CD11b (101,207, BioLegend), APC/Cyanine7 anti-Ly6C (128,025, BioLegend), Brilliant violet 421 anti-CD45 (103,134, BioLegend), Biotin anti-CD3 (100,243, BioLegend), Biotin anti-TER119 (116,203, BioLegend), Biotin anti-Ly6G (127,603, BioLegend), and PerCP-Cyanine5.5 streptavidin (405,214, BioLegend). To exclude dead cells from analysis, cells were stained with Fixable Viability Stain 700 (564,997, BD Biosciences). Cells were analyzed and sorted using a Cell Sorter SH800S (Sony). Data were processed with FlowJo (v10) (Tree Star).

Electrical stimulation-induced paw withdrawal test

The electrical stimulation-induced paw withdrawal test was performed as previously described [29]. Briefly, mice were placed in a polypropylene chamber without anesthesia and the left hind paw of each mouse was drawn thorough a hole in the chamber. After 5 min, electrodes (3 mm in diameter) were fastened to the left plantar surface and instep of the hind paw of each mouse. Transcutaneous nerve stimuli using each of three sine wave currents (5, 250, and 2000 Hz) were applied for 3 s through the electrodes. The current intensity was increased gradually, and the minimum current intensity of the paw withdrawal response was defined as the current stimulus threshold. Transcutaneous nerve stimuli using each sine wave current were applied at 5-min intervals. The same measurements were repeated 3–4 times for the same mouse on the experiment day and the next day (at 4-h intervals within a day). The paw withdrawal threshold was averaged from 3–4 measurements per paw. The experimenter was blinded to the genotype of the mice.

Quantification and statistical analysis

Quantifications were performed from at least three independent experimental groups. Data are presented as mean ± SEM. Statistical analyses were performed using Student's *t*-test or Welch's *t*-test for two groups, or one-way ANOVA for multiple groups, and significant differences between group means were identified with the Tukey–Kramer test. All statistical tests were two-tailed and $p < 0.05$ was considered significant. Statistical significance is indicated as asterisks: $^*p < 0.05$, $^{**}p < 0.01$. All n values are indicated in figure legends. Sample size was determined to be adequate based on the magnitude and consistency of measurable differences between groups. We confirmed that replicate experiments were successful by repeating at least three times for all experiments.

Data availability

All data supporting the findings of this study are found within the manuscript and its Supplementary information, and are available from the corresponding author upon reasonable request.

Received: 10 June 2024; Accepted: 4 November 2024
Published online: 08 November 2024

References

1. Abraira, V. E. & Ginty, D. D. The sensory neurons of touch. *Neuron* https://doi.org/10.1016/j.neuron.2013.07.051 (2013).
2. Basbaum, A. I., Bautista, D. M., Scherrer, G. & Julius, D. Cellular and Molecular Mechanisms of Pain. *Cell* https://doi.org/10.1016/j.cell.2009.09.028 (2009).
3. Cain, D. M., Khasabov, S. G. & Simone, D. A. *Response Properties of Mechanoreceptors and Nociceptors in Mouse Glabrous Skin: An In Vivo Study*. www.jn.physiology.org (2001).
4. Li, L. et al. The functional organization of cutaneous low-threshold mechanosensory neurons. *Cell* **147**, 1615–1627 (2011).
5. Olson, W., Dong, P., Fleming, M. & Luo, W. The specification and wiring of mammalian cutaneous low-threshold mechanoreceptors. *Wiley Interdiscip Rev Dev Biol* **5**, 389–404 (2016).
6. Tanaka, T. et al. Dermal macrophages set pain sensitivity by modulating the amount of tissue NGF through an SNX25–Nrf2 pathway. *Nat Immunol* **24**, 439–451 (2023).
7. Cullen, P. J. & Korswagen, H. C. Sorting nexins provide diversity for retromer-dependent trafficking events. *Nature Cell Biology* https://doi.org/10.1038/ncb2374 (2012).

8. Barker, P. A., Mantyh, P., Arendt-Nielsen, L., Viktrup, L. & Tive, L. Nerve growth factor signaling and its contribution to pain. *Journal of Pain Research* https://doi.org/10.2147/JPR.S247472 (2020).
9. Stratiievska, A. et al. Reciprocal regulation among TRPV1 channels and phosphoinositide 3-kinase in response to nerve growth factor. *Elife* https://doi.org/10.7554/eLife.38869.001 (2018).
10. Hefti, F. F. et al. Novel class of pain drugs based on antagonism of NGF. *Trends in Pharmacological Sciences* https://doi.org/10.1016/j.tips.2005.12.001 (2006).
11. Lumpkin, E. A. & Caterina, M. J. Mechanisms of sensory transduction in the skin. *Nature* https://doi.org/10.1038/nature05662 (2007).
12. Middleton, S. J. et al. Nav.17 is required for normal C-low threshold mechanoreceptor function in humans and mice. *Brain* **145**, 3637–3653 (2022).
13. Chakarov, S. et al. Two distinct interstitial macrophage populations coexist across tissues in specific subtissular niches. *Science* https://doi.org/10.1126/science.aau0964 (2019).
14. Kiermayer, C., Conrad, M., Schneider, M., Schmidt, J. & Brielmeier, M. Optimization of spatiotemporal gene inactivation in mouse heart by oral application of tamoxifen citrate. *Genesis (United States)* **45**, 11–16 (2007).
15. Tatsumi, K. et al. Olig2-Lineage astrocytes: A distinct subtype of astrocytes that differs from GFAP astrocytes. *Front Neuroanat* https://doi.org/10.3389/fnana.2018.00008 (2018).
16. Kolter, J. et al. A Subset of Skin Macrophages Contributes to the Surveillance and Regeneration of Local Nerves. *Immunity* **50**, 1482-1497.e7 (2019).
17. Tamoutounour, S. et al. Origins and functional specialization of macrophages and of conventional and monocyte-derived dendritic cells in mouse skin. *Immunity* **39**, 925–938 (2013).
18. Baral, P. et al. Nociceptor sensory neurons suppress neutrophil and γδ T cell responses in bacterial lung infections and lethal pneumonia. *Nat Med* **24**, 417–426 (2018).
19. Tomlinson, R. E. et al. NGF-TrkA signaling in sensory nerves is required for skeletal adaptation to mechanical loads in mice. *Proc Natl Acad Sci U S A* **114**, E3632–E3641 (2017).
20. Keeler, A. B. et al. A developmental atlas of somatosensory diversification and maturation in the dorsal root ganglia by single-cell mass cytometry. *Nat Neurosci* **25**, 1543–1558 (2022).
21. Crawford, L. T. K. & Caterina, M. J. Functional Anatomy of the Sensory Nervous System: Updates From the Neuroscience Bench. *Toxicol Pathol* **48**, 174–189 (2020).
22. Ren, K. & Dubner, R. Interactions between the immune and nervous systems in pain. *Nature Medicine* https://doi.org/10.1038/nm.2234 (2010).
23. Seal, R. P. et al. Injury-induced mechanical hypersensitivity requires C-low threshold mechanoreceptors. *Nature* **462**, 651–655 (2009).
24. Handler, A. & Ginty, D. D. The mechanosensory neurons of touch and their mechanisms of activation. *Nature Reviews Neuroscience* https://doi.org/10.1038/s41583-021-00489-x (2021).
25. van den Dries, K., Linder, S., Maridonneau-Parini, I. & Poincloux, R. Probing the mechanical landscape – new insights into podosome architecture and mechanics. *Journal of Cell Science* https://doi.org/10.1242/jcs.236828 (2019).
26. Alonso, F., Spuul, P., Daubon, T., Kramer, Ij. & Génot, E. Variations on the theme of podosomes: A matter of context. *Biochimica et Biophysica Acta - Molecular Cell Research* https://doi.org/10.1016/j.bbamcr.2018.12.009 (2019).
27. Foster, P. A., Costa, S. K. P., Poston, R., Hoult, J. R. S. & Brain, S. D. Endothelial cells play an essential role in the thermal hyperalgesia induced by nerve growth factor. *The FASEB journal : official publication of the Federation of American Societies for Experimental Biology* **17**, 1703–1705 (2003).
28. Yamazaki, D. et al. The Mg2+ transporter CNNM4 regulates sperm Ca2+ homeostasis and is essential for reproduction. *J Cell Sci* **129**, 1940–1949 (2016).
29. Okuda-Ashitaka, E. et al. Mechanical allodynia in mice with tenascin-X deficiency associated with Ehlers-Danlos syndrome. *Sci Rep* https://doi.org/10.1038/s41598-020-63499-2 (2020).

Acknowledgements

This work was supported by JSPS KAKENHI (to TT, 23K06807), the Takeda Science Foundation (to TT), and the Mitsubishi Foundation (to TT). We thank Mrs. Tomoko Tada (Nara Medical University) for technical assistance. We thank Dr. Ian Smith for providing language help.

Author contributions

TT and AW conceived the project and designed the experiments. TT, AI, MB, RY, MS, EOA, HF, HO, and KT performed the experiments. TT, AI, MB, RY, MS, EOA and HF analyzed the data. TT and AW wrote the paper.

Declarations

Competing interests

All authors have no affiliations with or involvement in any organization or entity with any financial interest, or non-financial interest, in the subject matter or materials discussed in this manuscript. The authors declare no competing interests.

Additional information

Supplementary Information The online version contains supplementary material available at https://doi.org/10.1038/s41598-024-78683-x.

Correspondence and requests for materials should be addressed to T.T.